Electronic Supplementary Material (ESI) for Journal of Materials Chemistry A.

Coupling Electrocatalytic Redox-Active Sites in Three-Dimensional Bimetalloporphyrin-based Covalent Organic Framework for Enhancing Carbon Dioxide Reduction and Oxygen Evolution

Jie Li[ab], Yan-Xi Tan[acd], Jing Lin[ad], Yangyang Feng[ac], Xiang Zhang[acd], Enbo Zhou[ac], Daqiang Yuan[abcd] and Yaobing Wang[abcd]**

[a] CAS Key Laboratory of Design and Assembly of Functional Nanostructures, and Fujian Provincial Key Laboratory of Nanomaterials, State Key Laboratory of Structural Chemistry, Fujian Institute of Research on the Structure of Matter, Chinese Academy of Sciences, Fuzhou 350002, Fujian, P. R. China.

[b] College of Chemistry and Materials Science, Fujian Normal University, Fujian, Fuzhou 350007, China.

[c] University of Chinese Academy of Sciences, Beijing 100049, P. R. China.

[d] Fujian Science and Technology Innovation Laboratory for Optoelectronic Information of China, Fuzhou 350108, Fujian, P. R. China.

* Corresponding author: tyx@fjirsm.ac.cn; wangyb@fjirsm.ac.cn

1. Materials and Methods

Chemicals and reagents: Carbon paper (HCP-020, Hesen), Nafion membranes (Nafion 211, DuPont), bipolar membranes (TWBP, Astom). DI water was used in this work.

Co-TPNB-COF synthesis: A mixture of NBA (70 mg, 0.133 mmol), Co-TFP (78.2 mg, 0.1 mmol), *n*-BuOH (1.2 mL) and o-dichlorobenzene (*o*-DCB) (4.8 mL) in a 10 mL pyrex tube was sonicated for 10 min. The aqueous acetic acid (6 M, 0.6 mL) was added, and the mixture was sonicated to afford a homogeneous dispersion. The solution was transferred into and degassed by three freeze-pump-thaw cycles. The tube was sealed off and heated at 120 °C for 3 days. The solid was collected by filtration and washed with anhydrous DMF and EtOH. The powder was dried at 60 °C under vacuum overnight to afford **Co-TPNB-COF** as a dark brown solid (88.8 mg, 61.1%).

Ni-TPNB-COF synthesis: A mixture of NBA (70 mg, 0.133 mmol), Ni-TFP (78.2 mg, 0.1 mmol), *n*-BuOH (1.2 mL) and o-dichlorobenzene (*o*-DCB) (4.8 mL) in a 10 mL pyrex tube was sonicated for 10 min. The aqueous acetic acid (6 M, 0.6 mL) was added, and the mixture was sonicated to afford a homogeneous dispersion. The solution was transferred into and degassed by three freeze-pump-thaw cycles. The tube was sealed off and heated at 120 ^{o}C for 3 days. The solid was collected by filtration and washed with anhydrous DMF and EtOH. The powder was dried at 60 ºC under vacuum overnight to afford **Co-TPNB-COF** as a dark brown solid (81.8 mg, 56.3%).

Structure Simulation: Molecular modelling of the **Co/Ni-TPNB-COF** was performed using Materials Studio (version 7.0). Pawley refinement was performed using Reflex, a software package for crystal determination from PXRD patterns. The unit cell dimensions were set to the theoretical parameters. Pawley refinement was carried out to iteratively optimize the lattice parameters until the R_{wp} value converged and the superposition of the observed and refined profiles showed good agreement. The lattice models (e.g. cell parameters, atomic positions and total energies) were then fully optimized using the MS Forcite molecular dynamics module (universal force fields, Ewald summations).

DFT calculation. Geometry optimizations and the free energy calculations (base on Nørskov method[1]) were carried out by Vienna Ab-initio Simulation Package (VASP)[2]. In consideration of the efficient of the calculation and the geometry with large atoms, the model for single-point energy calculation and electronic structure calculations (include density of states and band decomposed charge density) was constructed as the fragment of 3D COF, which was two M-Tp linked and around by triphenylamine (Figure 2). Then the charge density difference of system is calculated by the following expressions: $\Delta\rho = \rho(\text{3D COF}) - \rho(\text{Ni-Tp}) - \rho(\text{Co-Tp}) - \rho(\text{TPA})$. The d-band center was determined by performing the projected density of states (PDOS) analysis, which involved the integration of the DOS for d orbitals up to the Fermi level. The cutoff energy was set as 500 eV with Gamma point. The energy and force convergence were 10^{-4} eV and 0.1 eV/Å, respectively. The electron spin interaction was also in consideration with the initial magnetic moment of Co (3.0) and Ni (0.0). The two-

electron CDRR process and the four-electron OER process were described as the following equations:

CDRR process:

Step1: * + $CO_2 \rightarrow$ *COO

Step2: *COO + $H^+ + e^- \rightarrow$ *$COOH$

Step3: *$COOH$ + $H^+ + e^- \rightarrow$ *CO + H_2O

Step4: *$CO \rightarrow$ * + CO

OER process:

Step5: * + $OH^- \rightarrow *OH + e^-$

Step6: $*OH + OH^- \rightarrow *O + H_2O + e^-$

Step7: $*O + OH^- \rightarrow *OOH + e^-$

Step8: $*OOH + OH^- \rightarrow * + O_2 + H_2O + e^-$

then the free energy of each step can be described by the following expressions:

$\Delta G1 = G(*COO) - G(*) - G(CO_2)$ - ΔpH - eU

$\Delta G2 = G(*COOH) - G(*COO) - G(H^+)$ - ΔpH - eU

$\Delta G3 = G(*CO) + G(H_2O) - G(*COOH) - G(H^+)$ - ΔpH - eU

$\Delta G4 = G(*) + G(CO) - G(*CO)$ - ΔpH - eU

$\Delta G5 = G(*OH) - G(OH^-) - G(*)$ - ΔpH - eU

$\Delta G6 = G(*O) + G(H_2O) - G(*OH) - G(OH^-)$ - ΔpH - eU

$\Delta G7 = G(*OOH) - G(*O) - G(OH^-)$ - ΔpH - eU

$\Delta G8 = G(M) + G(H_2O) + G(O_2) - G(*OOH) - G(OH^-)$ - ΔpH - eU

Where $G(H^+)$ can be replaced by $1/2G(H_2)$ and $G(OH^-)$ can be replaced by $G(H_2O) - 1/2\ G(H_2)$, considering the reaction of $H^+ + e^- = 1/2H_2$ and $H^+ + OH^- = H_2O$ is in equilibrium state at standard condition.

Calculation of Faradaic efficiency. The Faradaic efficiency (FE) for CO production at each applied potential was calculated based on the following equations: $FE = j_{CO}/j_{total} = v_{CO} \times N \times F/j_{total}$. FE: Faradaic efficiency for CO production (%); j_{CO}: partial current density for CO production; j_{total}: total current density; v_{CO}: the production rate of CO; N: the number of electrons transferred for product formation. Here, it is 2 for CO; F: Faradaic constant, 96485 C/mol.

Calculation of turnover frequency (TOF, s^{-1}). The TOF for CO was calculated based on the following equations: TOF = $j_{total} \times FE_{CO}/(N \times F \times n_{total} \times f)$. j_{total}: total current density; FE: Faradaic efficiency for CO production (%); N: the number of electron transferred for product formation (here, it is 2 for CO); F: Faradaic constant, 96485 C/mol; n_{total}: the total moles of catalyst employed in the electrolysis; *f*: the surface fraction of electrochemically active Co or Ni sites.

Determination of surface concentration of electroactive Co(II)-porphyrin units in Co/Ni-TPNB-COF. To estimate the surface concentration of electroactive Co(II)-porphyrin units in COFs, cyclic voltammetry tests of **Co/Ni-TPNB-COF** in Ar saturated 0.4 M $KHCO_3$ on the scan rate between 20 to 60 mV/s were conducted. The peak current shows a linear dependence on the scan rate. Calculation of surface coverage (τ_0) for **Co/Ni-TPNB-COF**: Regression of the linear regime between 20 and 60 mV/s with equation: slope = $n^2F^2A\tau_0/(4RT)$, where n is the number of electrons involved, F is the Faraday constant; A is geometrical surface area of the electrode (1 cm^2), τ_0 is the surface coverage, R is the gas constant, T is test temperature (298 K).

Characterization of gases: H_2 and CO production was detected by a gas chromatograph (GC, 9790II, FULI) equipped with a TDX-01 column, a Ni reformer, a thermal conductivity detector, and a hydrogen ion flame detector. O_2 generation was analyzed by a GC (9790II, FULI) equipped with a molecular 5A sieve column and a thermal conductivity detector.

Reference

[1] G. Kresse, J. Furthmuller, *Phys Rev B Condens Matter*, 1996, **54**, 11169-11186.
[2] J. Rossmeisl, Z. W. Qu, H. Zhu, G. J. Kroes, J. K. Nørskov, J. Electroanal. Chem., 2007, **607**, 83-89.

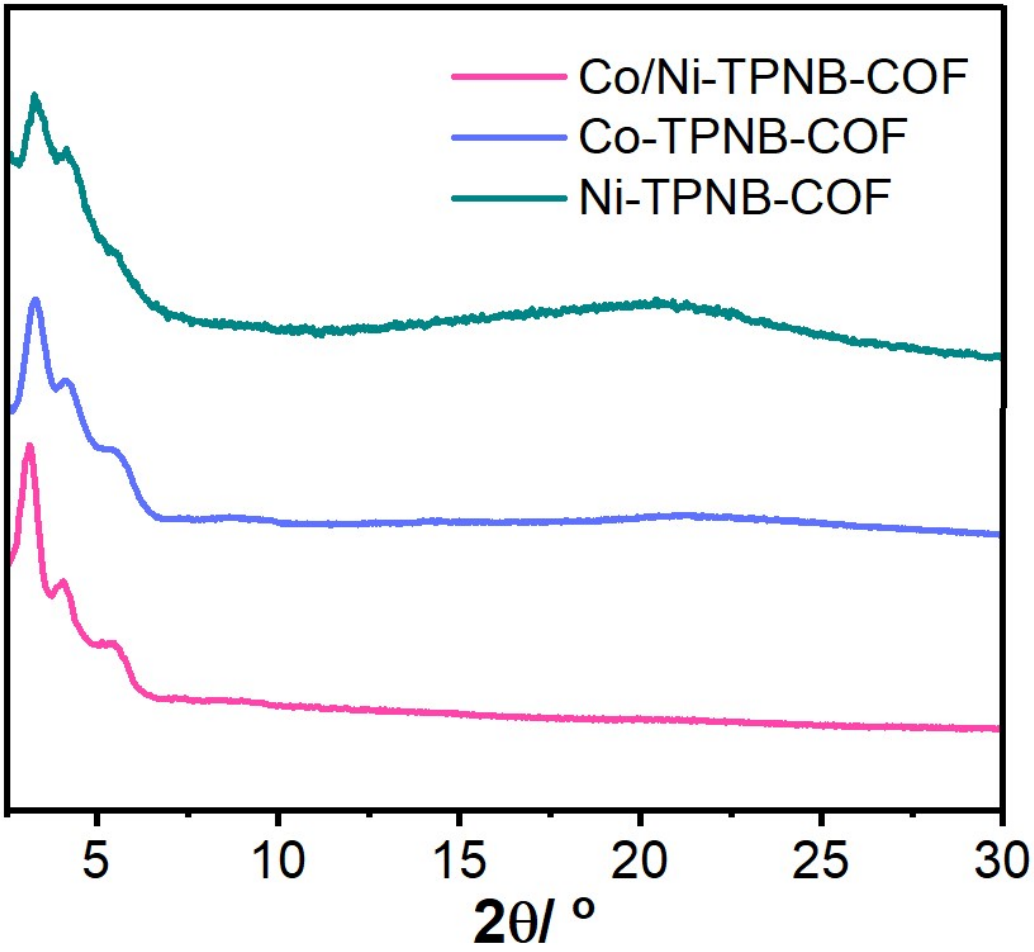

Figure S1. The PXRD patterns of three COFs.

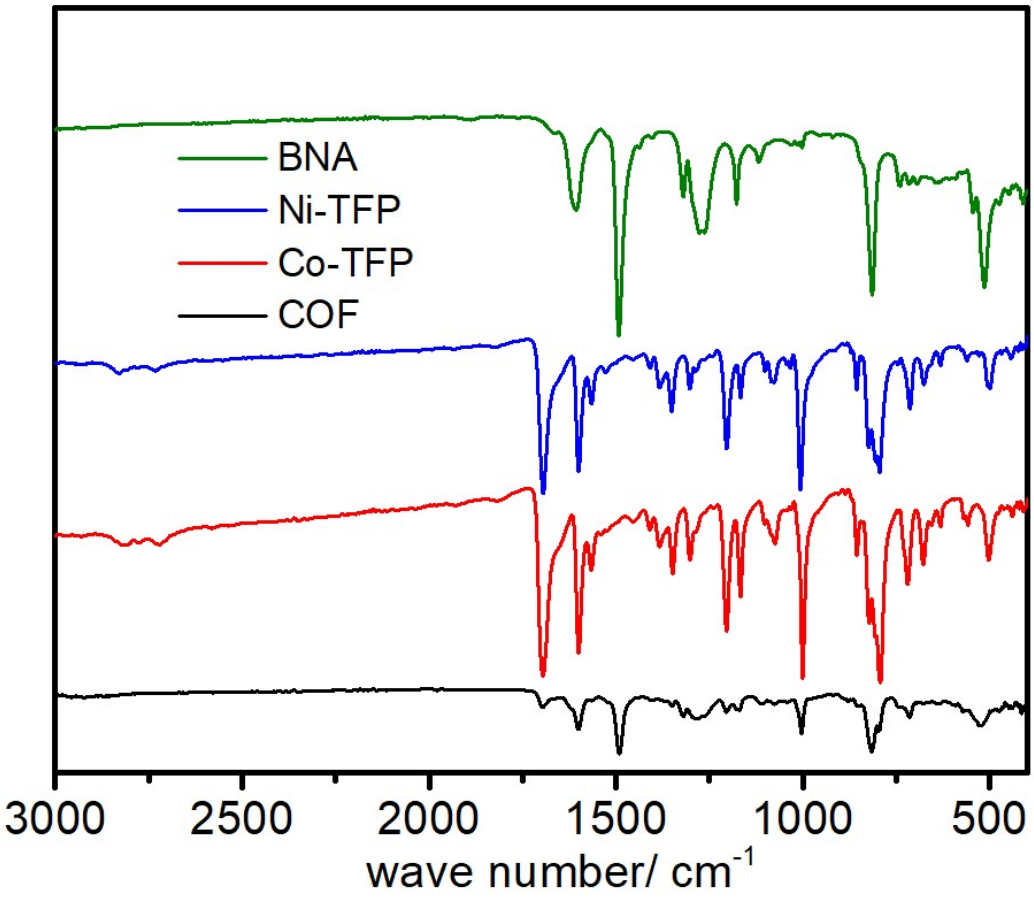

Figure S2. FT-IR spectra.

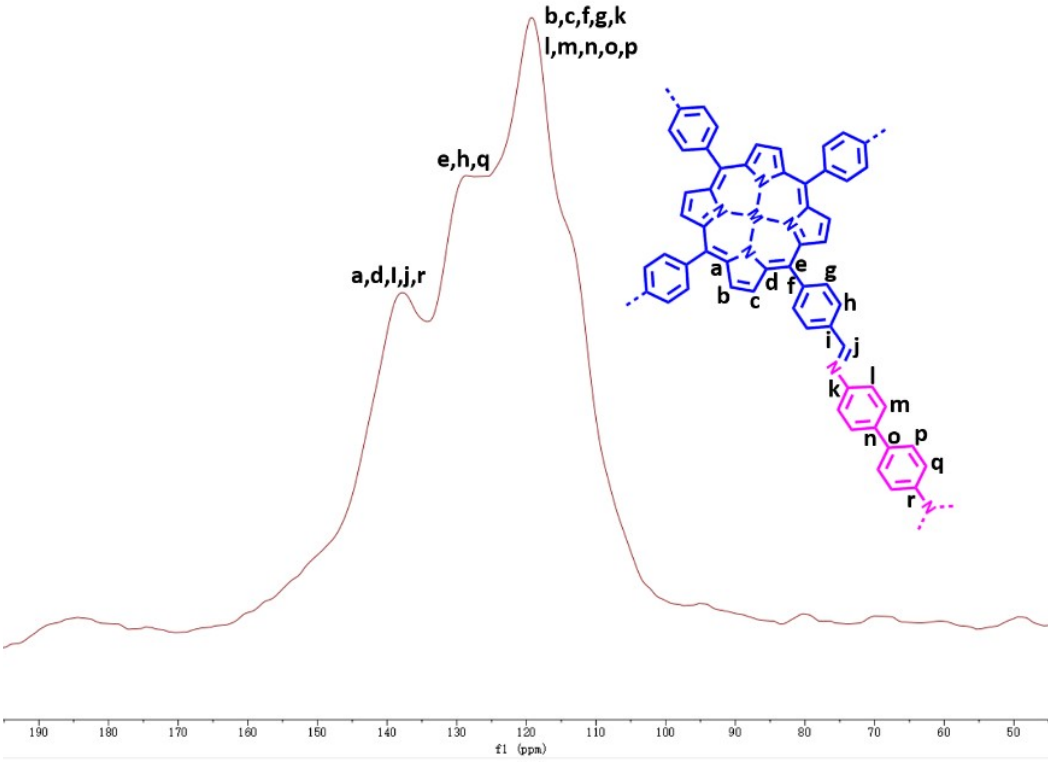

Figure S3. Solid-state ^{13}C NMR spectra of Co/Ni-TPNB-COF.

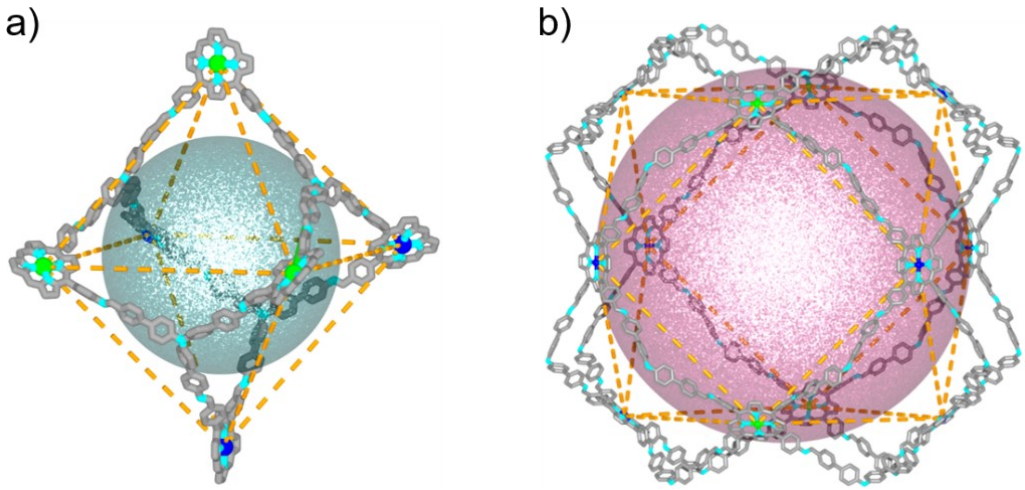

Figure S4. Octahedral (a) and cuboctahedral (b) cages in Co/Ni-TPNB-COF.

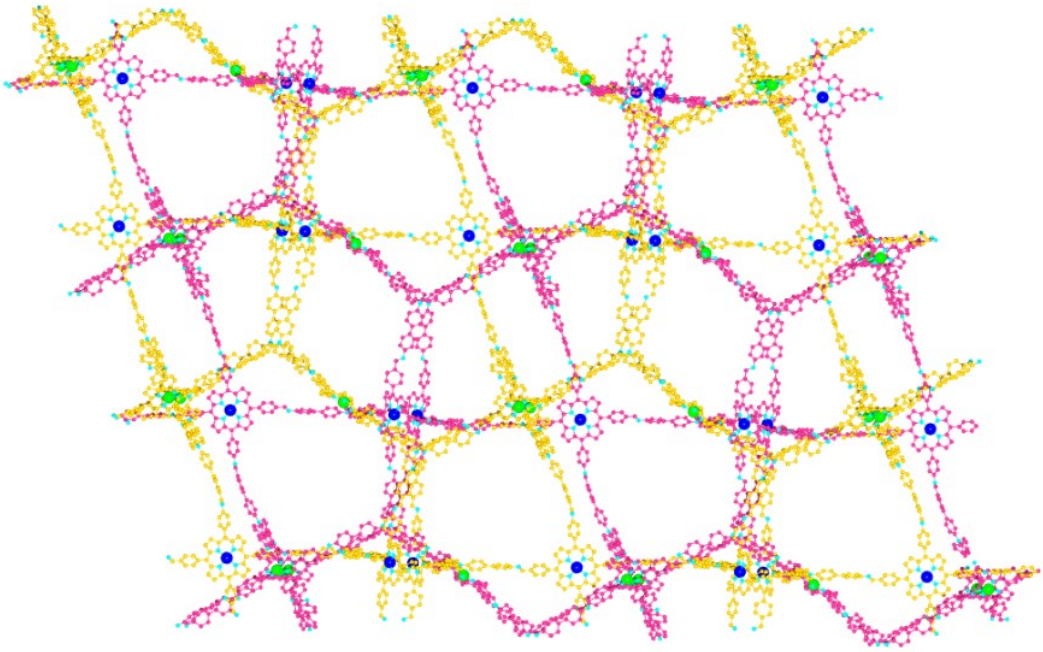

Figure S5. 2-fold interpenetrating *tbo* network of Co/Ni-TPNB-COF.

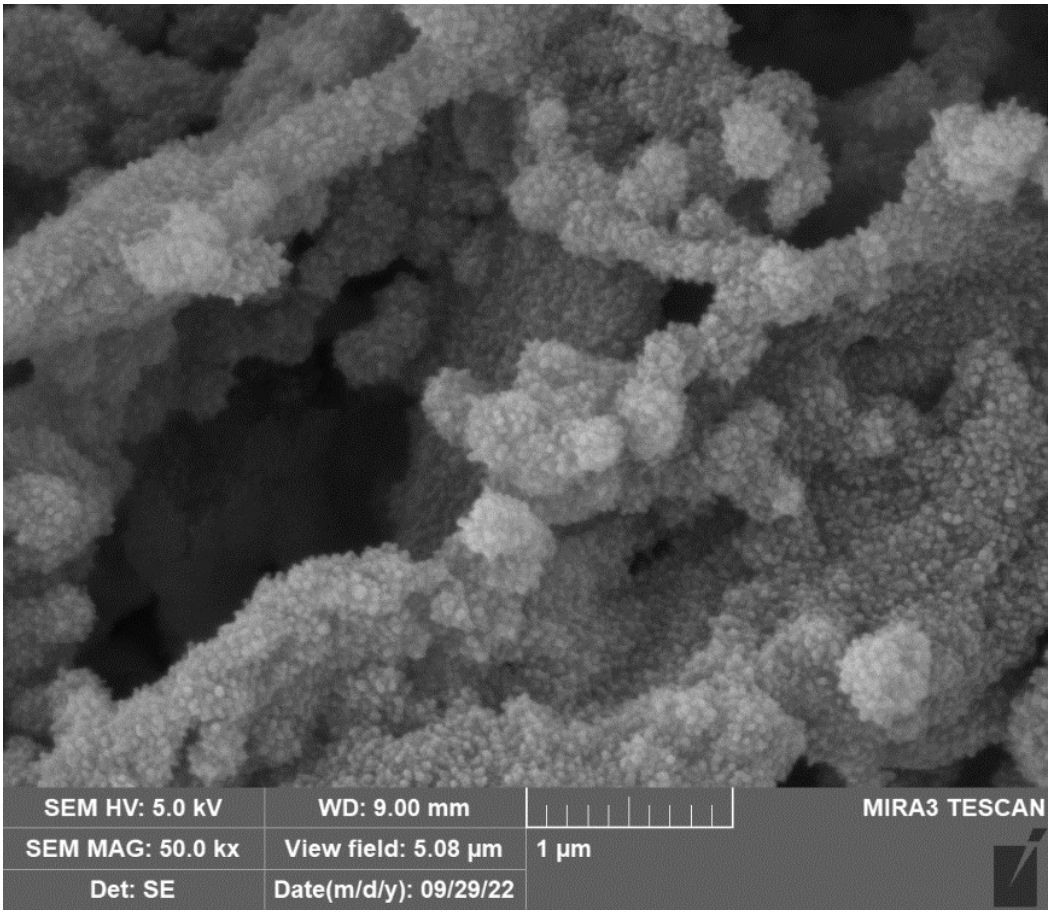

Figure S6. SEM images for Co/Ni-TPNB-COF.

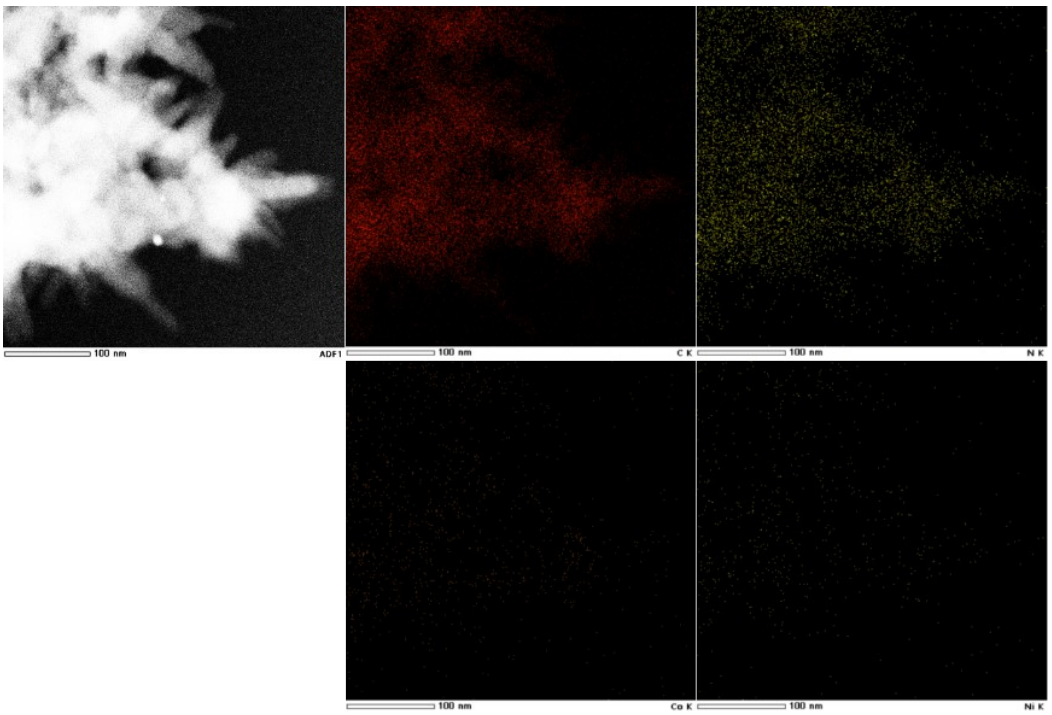

Figure S7. HAADF image and corresponding elemental mapping images.

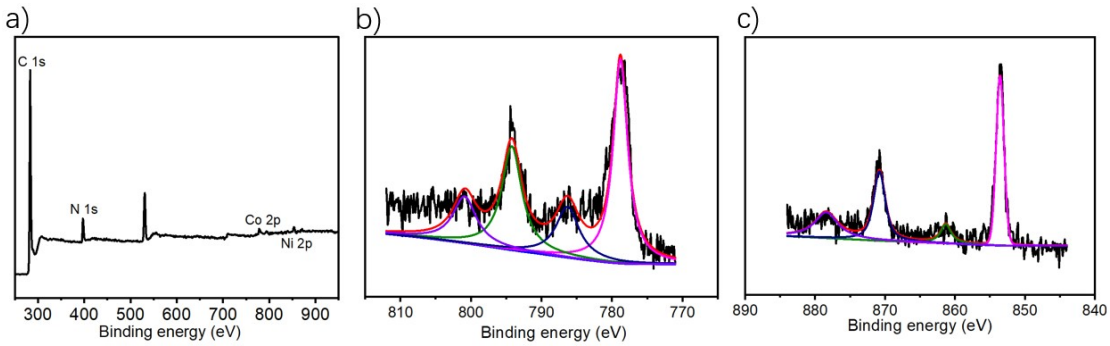

Figure S8. Total XPS spectrum (a), Co 2p (b) and Ni 2p (c) XPS spectrum of Co/Ni-TPNB-COF.

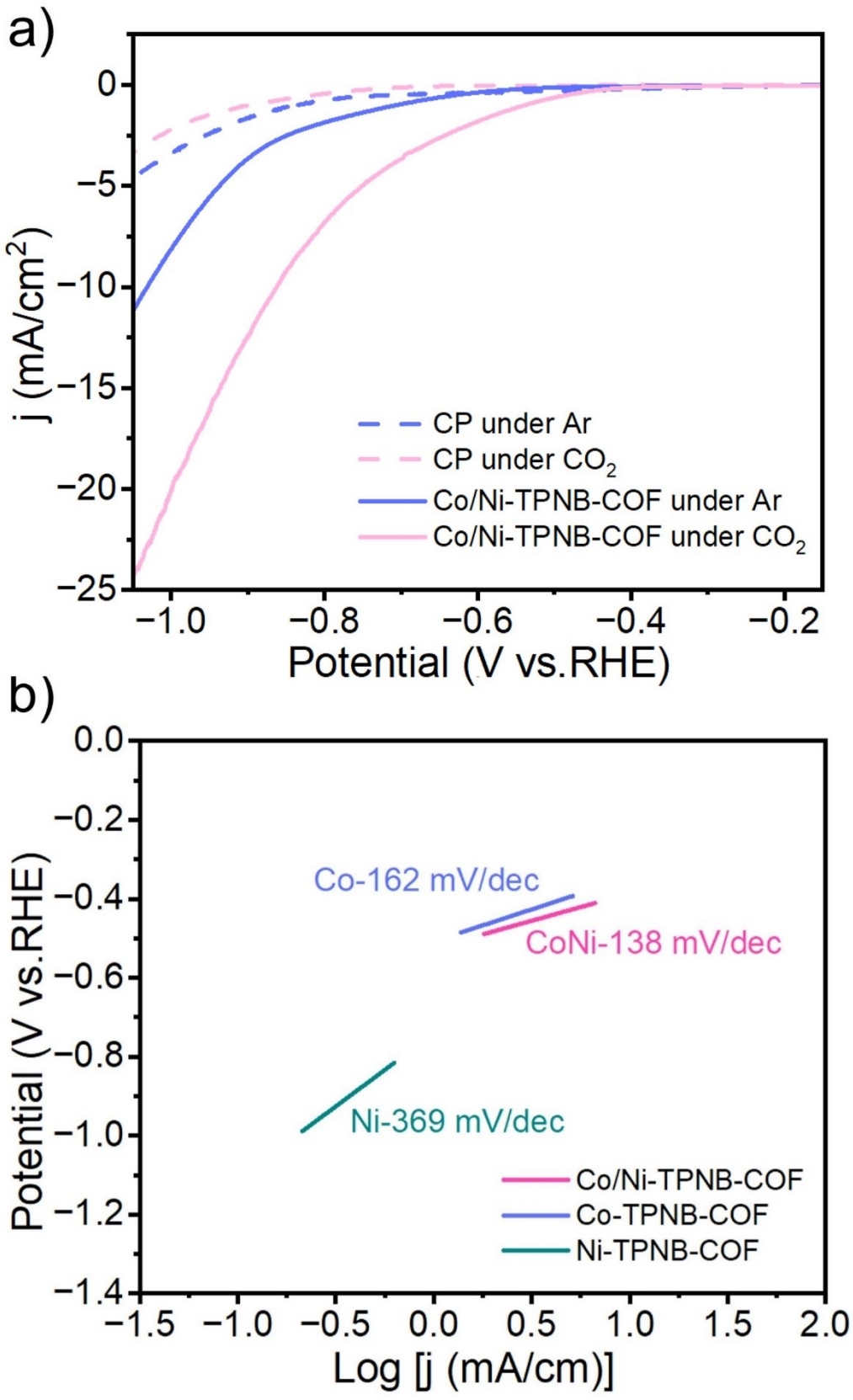

Figure S9. LSV curves (a) for electrochemical CDRR catalyzed by three COFs electrode and their corresponding Tafel plots (b).

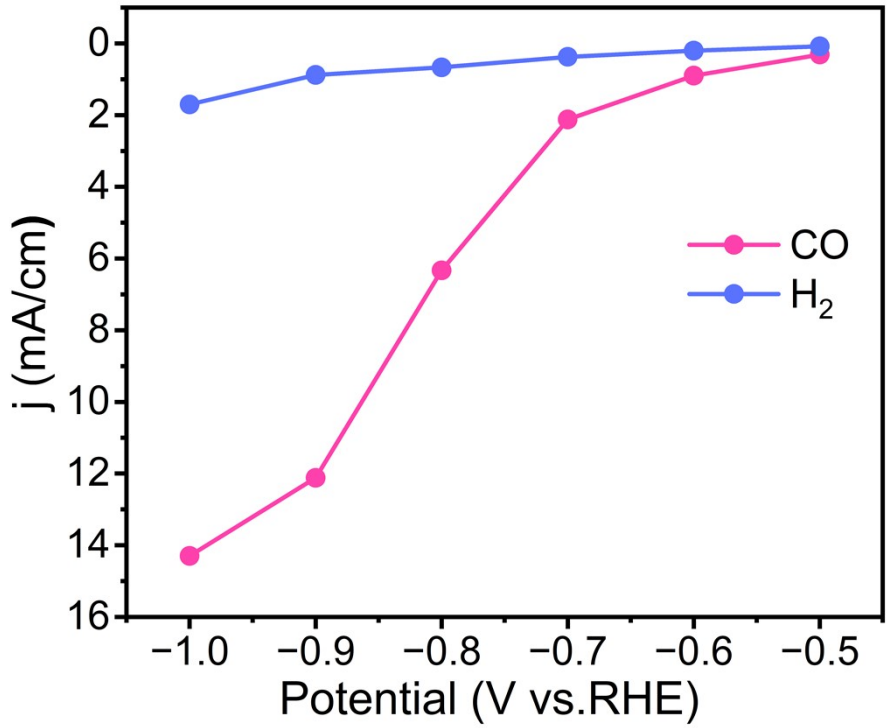

Figure S10. The partial current density of CO (j_{CO}) in potentiostatic electrolysis.

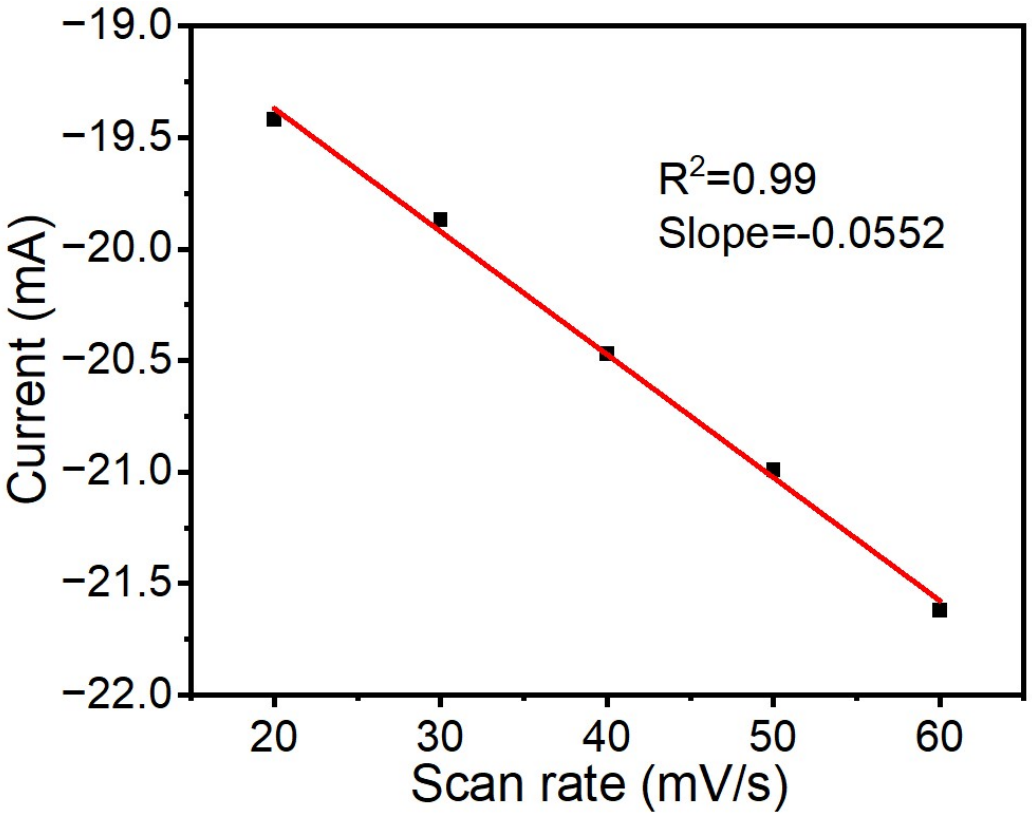

Figure S11. Peak current of the cyclic voltammogram of Co/Ni-TPNB-COF as a function of scan rate.

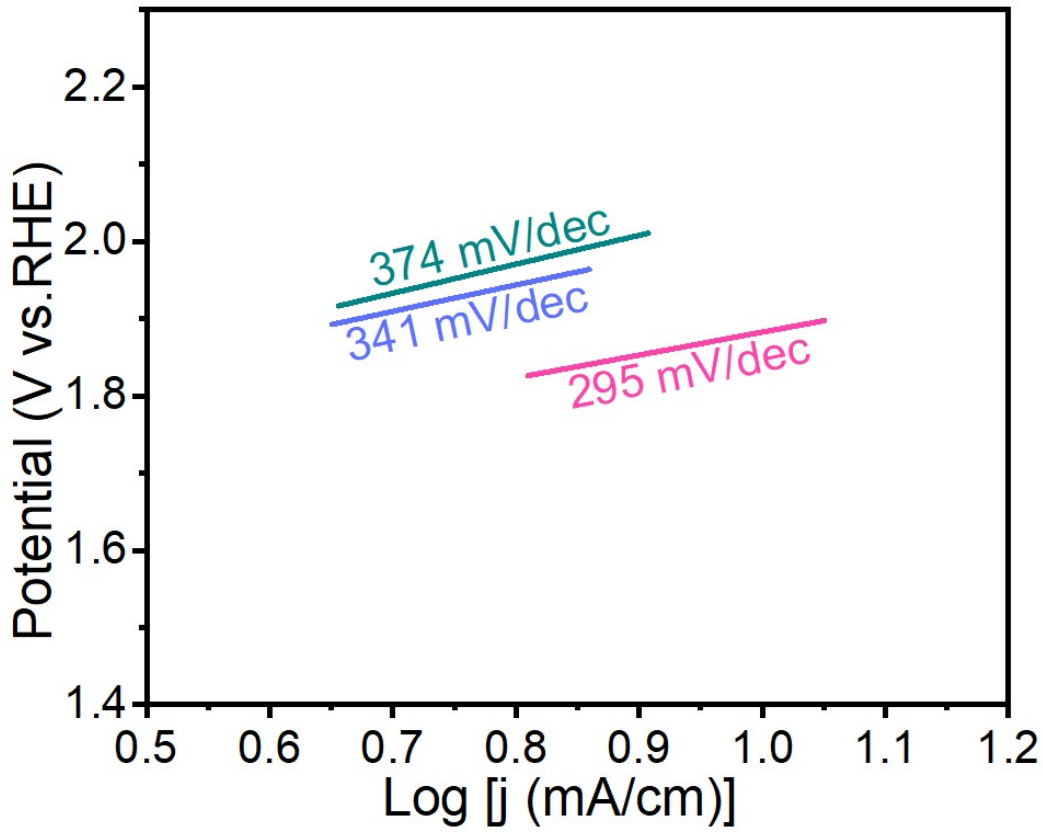

Figure S12. Tafel plots for the electrocatalytic OER catalyzed by **Co/Ni-TPNB-COF** (black), **Ni-TPNB-COF** (blue), **Co-TPNB-COF** (red).

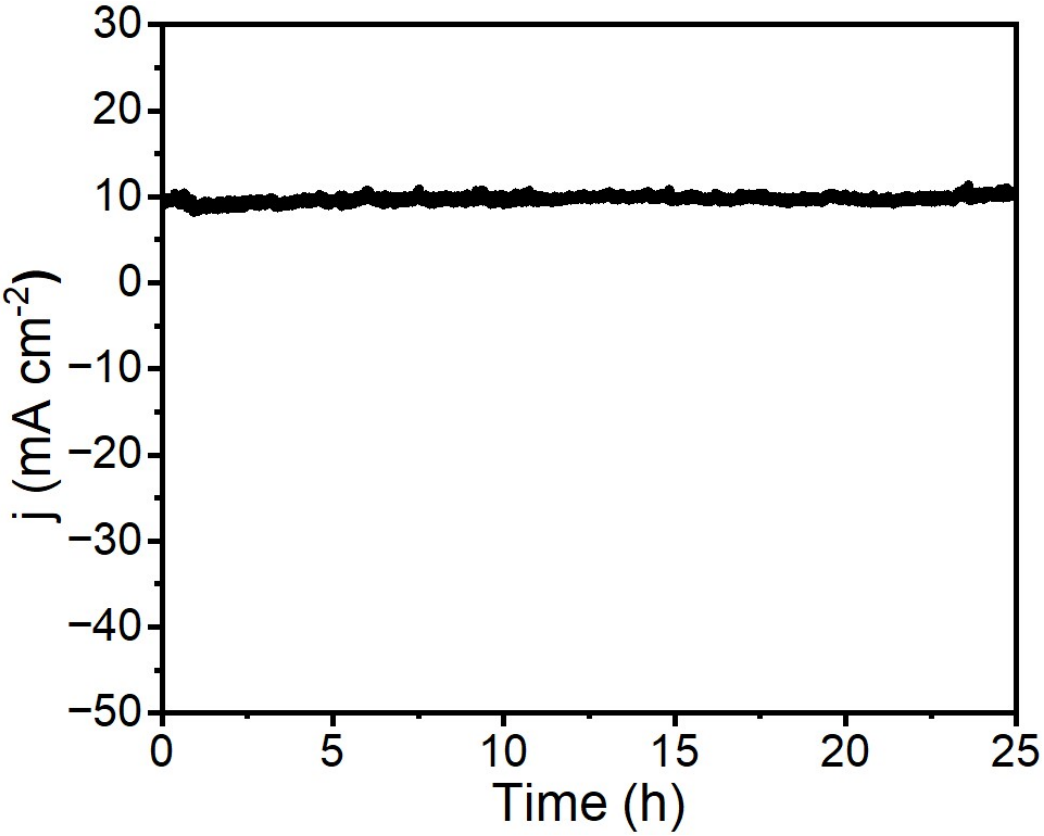

Figure S13. OER durability performance of Co/Ni-TPNB-COF electrode at the overpotential of 669 mV.

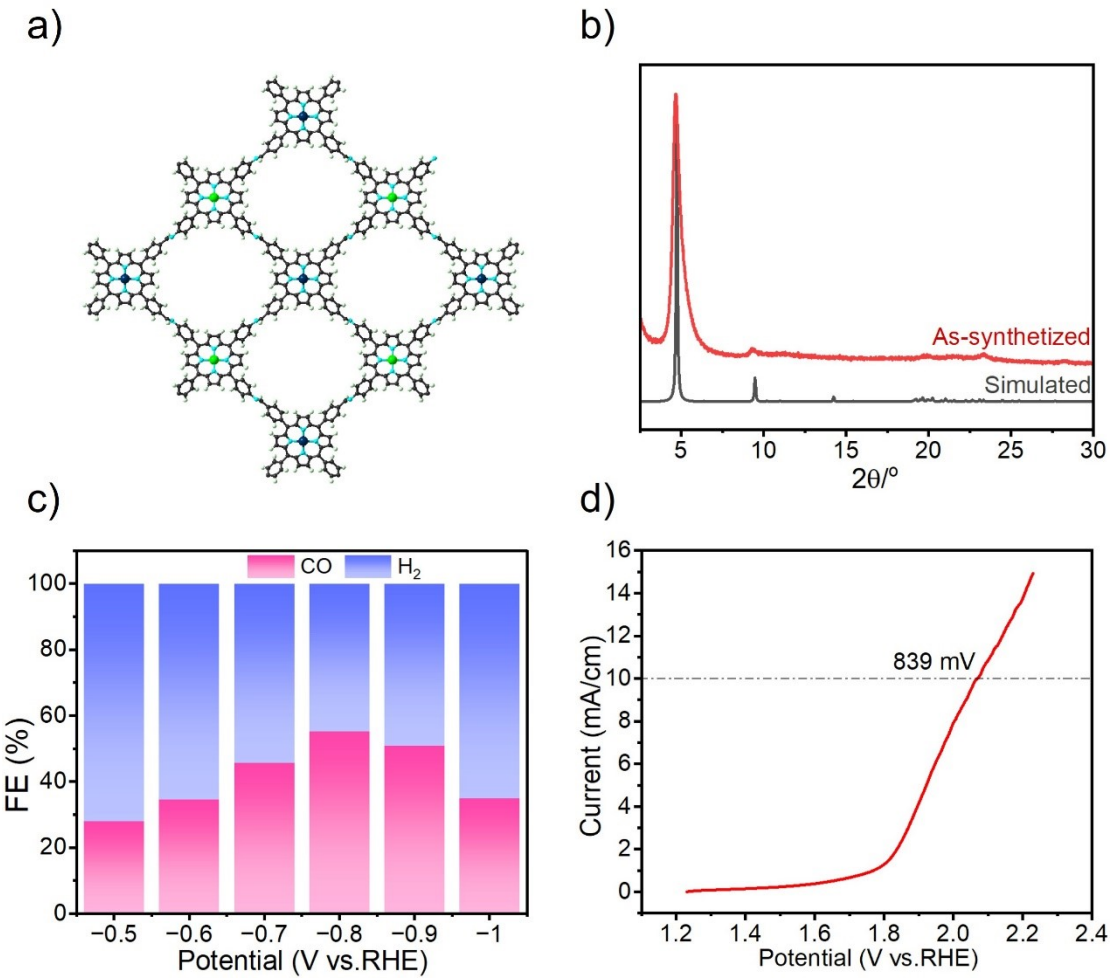

Figure S14 The information of Co/Ni-COF-420: a) the structure model, b) PXRD patterns, c) FE of CO and H_2 in potentiostatic electrolysis for the electrocatalytic CDRR, d) LSV curves for the electrocatalytic OER.

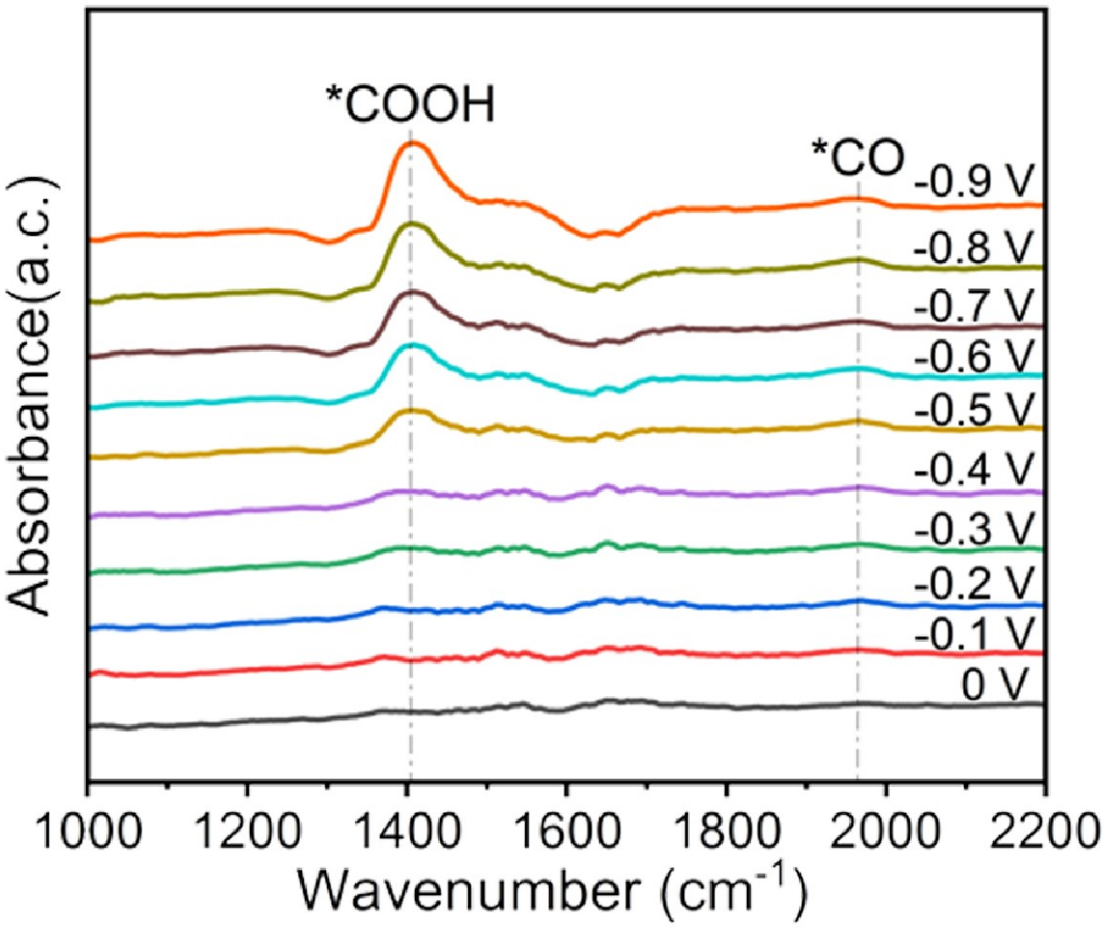

Figure S15 The situ electrochemical Fourier transform infrared spectroscopy (FTIR) during electrocatalytic CDRR catalyzed Co/Ni-TPNB-COF.

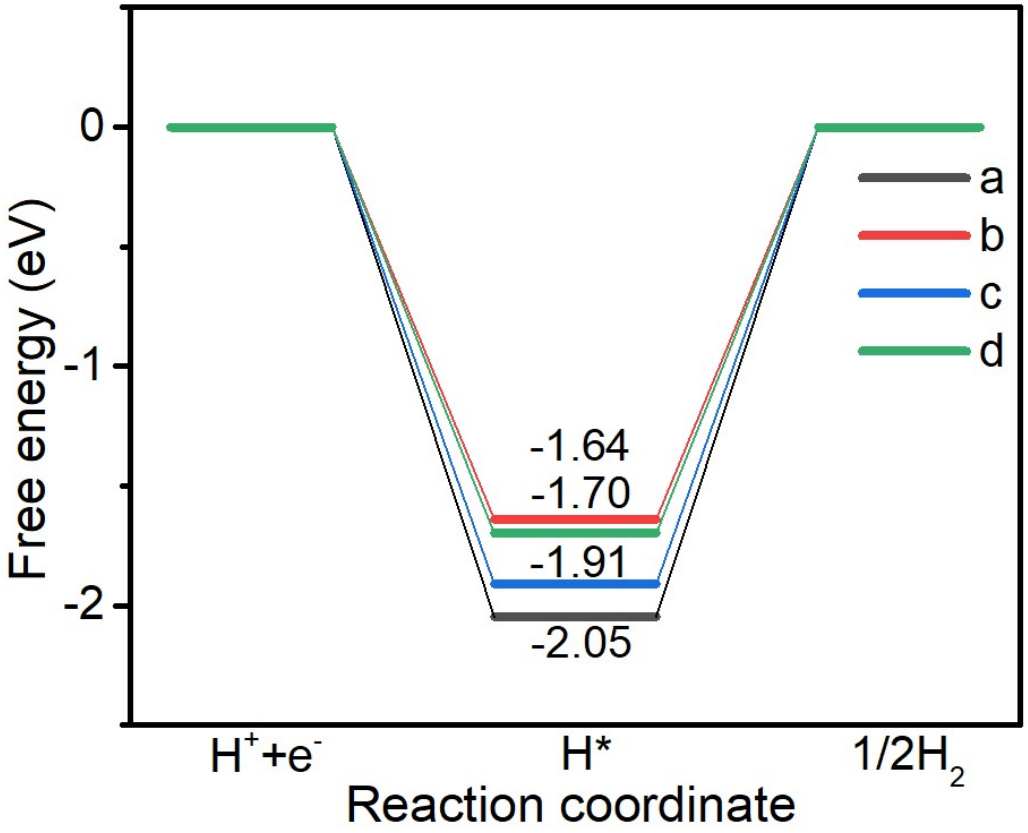

Figure S16. The free energy profles for CDRR (a) and OER (b) processes on the metal centers of Co/Ni-TPNB-COF (grey for Ni and red for Co), Co-TPNB-COF (blue) and Ni-TPNB-COF (green).

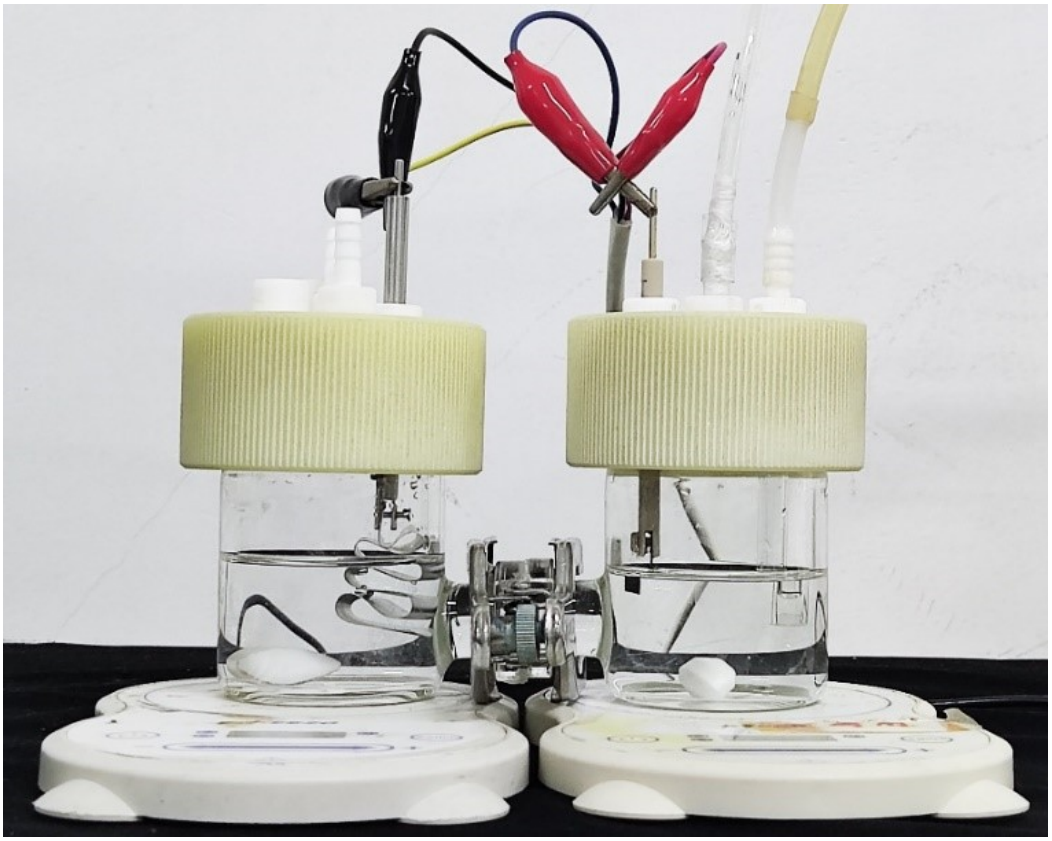

Figure S17. The photograph of Zn-CO_2 battery employed Co/Ni-TPNB-COF as cathode.

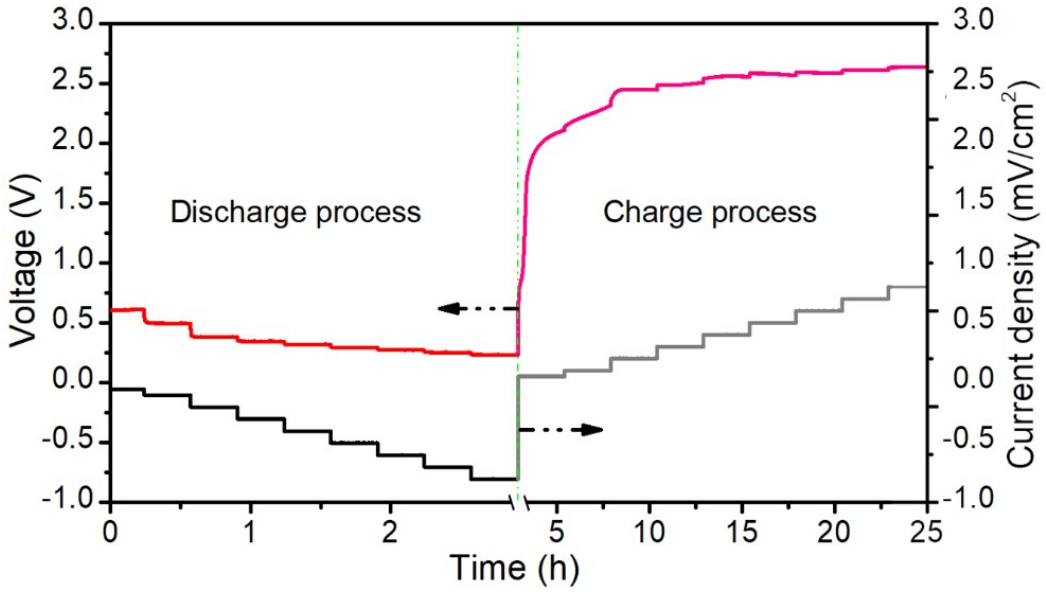

Figure S18. **Discharge and charge voltage curves under different current densities.**

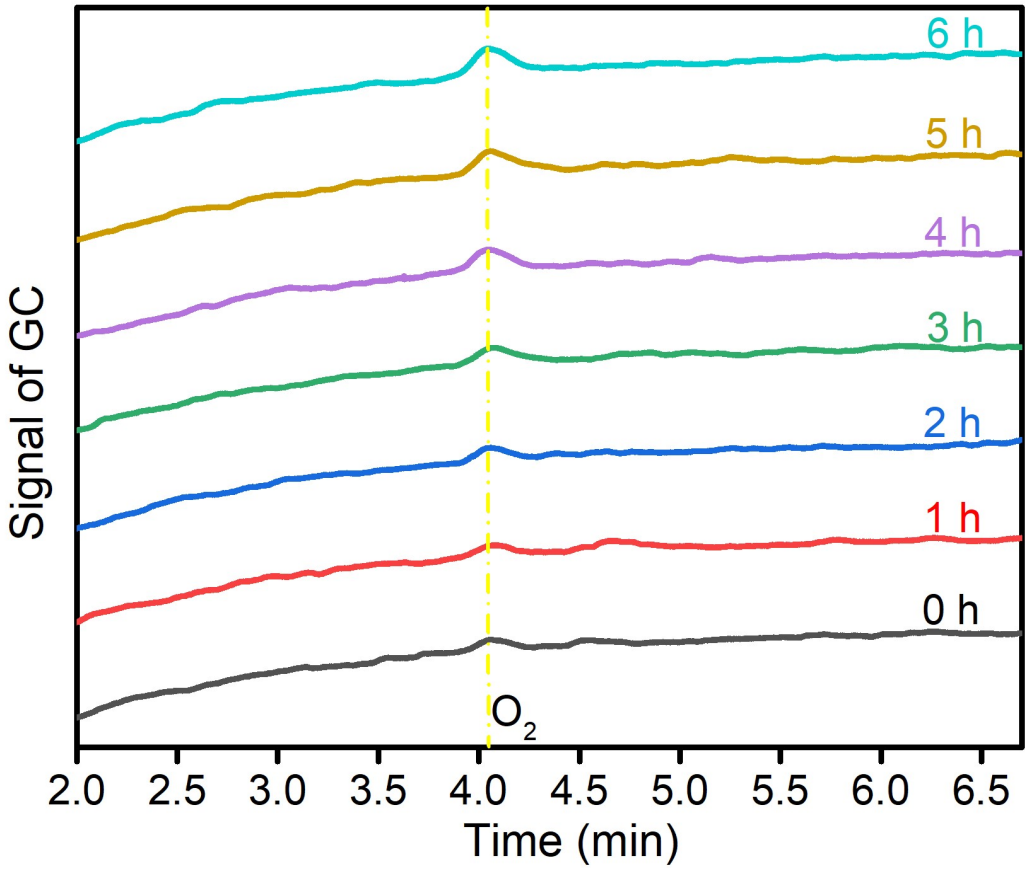

Figure S19. Signal intensity in GC of O_2 generation on Co/Ni-TPNB-COF dendrites during the cell charge.

Table S1 EE and of the aqueous rechargeable Zn-CO_2 electrochemical battery.

Current density (mA/cm^2)	Discharge voltage (V)	FE of $CO_2 \rightarrow CO + 1/2O_2$	FE of $H_2O \rightarrow H_2 + 1/2O_2$	Charge voltage (V)	EE (%)	EE' (%)
0.05	0.613	0.743	0.257	2.114	75.88	90.35
0.10	0.496	0.777	0.223	2.322	66.00	77.43
0.20	0.383	0.811	0.189	2.454	59.69	68.85
0.30	0.346	0.832	0.168	2.511	57.98	65.94
0.40	0.319	0.820	0.180	2.565	55.08	63.43
0.50	0.294	0.799	0.201	2.586	52.59	61.83
0.60	0.273	0.790	0.210	2.595	51.13	60.76
0.70	0.253	0.780	0.220	2.620	49.37	59.36
0.80	0.234	0.765	0.235	2.642	47.48	58.07

Note: EE is calculated based on CO_2 splitting in the battery; EE' is calculated based on both CO_2 splitting and water splitting.